

Thin front propagation in steady and unsteady cellular flows

M. Cencini^(a,b), A. Torcini^(a,c), D. Vergni^(a,b) and A. Vulpiani^(a,b)

- (a) Dipartimento di Fisica, Università "La Sapienza", Piazzale Aldo Moro 2, I-00185 Roma, Italy
(b) Istituto Nazionale di Fisica della Materia, UdR and SM C Roma 1, Piazzale Aldo Moro 2, I-00185 Roma, Italy
(c) Dipartimento di Energetica "S. Stecco", Via S. Marta, 3 - I-50139 Firenze, Italy

Front propagation in two dimensional steady and unsteady cellular flows is investigated in the limit of very fast reaction and sharp front, i.e. in the geometrical optics limit. In the steady case, by means of a simplified model, we provide an analytical approximation for the front speed, v_f , as a function of the stirring intensity, U , in good agreement with the numerical results. The main contribution to v_f comes from the large scale dynamics and, for sufficiently high U -values, $v_f = \ln U$ closely resembling the behavior proposed for turbulent flows. In the unsteady (time-periodic) case, the front speed displays a phase-locking on the flow frequency and, albeit the Lagrangian dynamics is chaotic, chaos in front dynamics only survives for a transient. Asymptotically the front dynamics is periodic and chaos manifests only in the spatially wrinkled structure of the front.

I. INTRODUCTION

Front propagation in fluid flows is relevant to many fields of sciences and technology ranging from marine ecology [1] to chemistry [2] and combustion technology [3]. A complete description of the problem would require to consider the coupled evolution of reactants and velocity field, including the back-reaction on the latter. This is typically a very difficult task [4]. Here we consider a simplified, but still physically significant, problem by assuming that the velocity field is not influenced by the reactants. In this respect, aqueous auto-catalytic reactions, and gaseous combustion with a large flow intensity but sufficiently low values of gas expansion across the flame are important chemical-physical systems which are not too far from this idealized situation [5].

In the simplest model one considers a scalar field, $(r;t)$, which represents the fractional concentrations of the reaction's products (i.e., $r = 1$ indicates inert material, $r = 0$ fresh one and $0 < r < 1$ means that fresh material coexists with products), evolving accordingly to the advection-reaction-diffusion equation [6,7]:

$$\partial_t r + u \cdot \nabla r = D_0 \nabla^2 r + f(r); \quad (1)$$

where D_0 is the molecular diffusivity, and u is a given incompressible ($\nabla \cdot u = 0$) velocity field. The term $f(r)$ describes the production process with its typical time scale τ .

Two limit cases of Eq. (1) are very well studied: $\tau \rightarrow 0$ and $u \rightarrow 0$. In the former the evolution equation for a passive scalar is recovered (for a review see Refs. [8]), but being this limit singular (because in this case h is a conserved quantity) it is not very useful. The latter corresponds to consider a medium at rest and Eq. (1) reduces to the reaction-diffusion equation. A huge literature (see e.g. Ref. [7] and references therein) originated by the seminal works of Fisher and Kolmogorov-

Petrovsky-Piskunov (FKPP) [9] is devoted to this specific subject.

One can study Eq. (1) for different geometries and boundary conditions. Here we always consider an infinite strip in the x -direction with a reservoir of fresh material on the right and inert products on the left, in the transverse direction we assume periodic boundary conditions. With this geometry one has a front of inert material (stable phase) propagating from left to right. If the medium is at rest with the FKPP production term, $f(r) = r(1-r)$, the front propagates with an asymptotic speed and thickness given by [7,9]

$$v_0 = 2 \sqrt{D_0}; \quad \delta = \frac{D_0}{c}; \quad (2)$$

where c is a constant depending on the definition adopted for δ . This result is valid whenever $f(r)$ is a convex function ($f'' < 0$) with $f(0) = f(1) = 0$ and $f'(0) = 1$. For non-convex $f(r)$ only an upper and lower bound for the front speed can be provided [7].

A more interesting physical situation is when the velocity field is non zero ($u \neq 0$). In general the front propagates with an average limiting speed, v_f , enhanced with respect to the fluid at rest ($v_f > v_0$). In the case of very slow reaction, by means of homogenization techniques [8], one can show that the front speed behaves as in Eq. (2) with D_0 replaced by a renormalized diffusion coefficient, D_e , the so-called eddy diffusivity (see Ref. [8] for an exhaustive review on the determination of the eddy-diffusivity). However, to our knowledge, a general method to compute v_f for a generic velocity field does not exist.

In realistic systems, the reaction time scale is of the same order or (more frequently) faster than the velocity time scale (fast reaction). In this case a simple renormalization of D_0 is typically not sufficient to encompass the dynamical properties of the system [10]. In some cases the front speed can be still obtained by Eq. (2) renor-

realizing not only the diffusion constant, $D_0 \ll D_e$, but also the reaction time τ_{eff} [11].

In this paper we are interested in the limit of very fast reaction and very thin front, i.e., in the so-called geometrical optics regime [5]. Formally, this corresponds to the limit $\tau \rightarrow 0, D_0 \rightarrow 0$ maintaining the ratio $D = \text{constant}$ [12]. Therefore, from (2), one has v_0 finite and $\tau \rightarrow 0$. In this regime the front is well identified as a surface (a line in 2d), and the effect of the velocity field is to wrinkle the front increasing its area (length in 2d) and thereby its speed (see Eq. (3) of Sect. II). Concerning the velocity field we consider steady and unsteady cellular flows (i.e., with closed stream lines) in two-dimensions [13,15,16].

Cellular flows are interesting for many aspects. Since in real hydrodynamical systems coherent structures are typically present, cellular flows offer an idealized (but non-trivial) paradigm for studying front dynamics in realistic flows. We will also consider the presence of small scale spatial structures in the velocity field in order to investigate their possible role. This is a necessary step, even if still insufficient, toward the problem of front propagation in turbulent flows.

Concerning unsteady cellular flows, it is natural to ask for the possible influence of Lagrangian chaos [17] (when it is present) on front propagation. Moreover, it is interesting to compare the front speed for time dependent cellular flows with the one obtained for time dependent shear flows. Recent works [18-20] on the latter have shown that time dependence may cause a bending of the front speed, i.e., a depletion of the speed enhancement with respect to the steady case. We will see that some kind of time (periodic) dependence can produce rather subtle effects, namely the front speed locks on the frequency of the flow: a phenomenon which goes under the name of mode-locking (or frequency-locking) [21,22], and which has been already found to be present in some models of front propagation [23].

The paper is organized as follows. In Section II we discuss some general results concerning fronts in the geometrical optics limit, and the problem of front propagation in cellular flows. Section III is dedicated to the study of front propagation in the case of time independent cellular flow. We propose a simple one dimensional model which well reproduces the numerical results. In Section IV time dependent cellular flows are investigated, considering the effects of Lagrangian chaos and the velocity phase-locking. Some final remarks are reported in Section V. The Appendixes are devoted to the numerical methods here employed and to a more detailed treatment of the frequency-locking phenomenon.

II. THE GEOMETRICAL OPTICS LIMIT

From a physical point of view the geometrical optics limit (in combustion jargon, the flamelet regime) corresponds to sufficiently fast chemistry and very thin reac-

tion regions compared to the small scales of the flow (e.g. in turbulent flows this means that the front thickness should be smaller than the Kolmogorov length scale λ_K , i.e. $\tau \ll \lambda_K$) [6]. Since the front is sharp, its dynamics can be described in terms of the evolution of the surface (line in 2d) which divides the region in which $\phi = 1$ (inert material) from the other in which $\phi = 0$ (fresh material).

In absence of stirring ($u = 0$) the front evolves according to the Huygens principle, i.e., a point x belonging to the front surface moves with a velocity $v(x) = v_0 \hat{n}(x)$, where $\hat{n}(x)$ is the perpendicular to the front surface in x . At large times the front surface is asymptotically close to a sphere (circle in 2d) if the boundary conditions are open. On the other hand the preasymptotic behavior can be interesting in some technological problems and its treatment is mathematically non trivial [24].

In presence of stirring ($u \neq 0$) the problem is much more difficult. Here we study a 2D system with transverse length L and infinite horizontal extension. We assume periodic boundary conditions in the transverse directions and by fixing $\phi = 1$ for $x \leq -1$ and $\phi = 0$ for $x \geq 1$ the front propagates from left to right.

The first attempts to determine the front speed in such a regime dates back to 40's to the work of Damköler [6] who suggested that if the velocity field does not change the local (bare) front speed, v_0 , then the effective front speed is proportional to the total front area divided by the cross-section flow area. In two-dimensional geometry this means:

$$v_f = v_0 = L_f / L \quad (3)$$

where L is the transverse length, v_f and L_f are the average front speed and length respectively, where instantaneous front velocity and length can be defined as follows. The instantaneous velocity $v(t)$ is given by

$$v(t) = \frac{1}{L} \int_{-1}^1 dy \int_{-1}^1 dx \partial_t \phi(x;y;t) \quad (4)$$

In order to define the front length, L , we introduce the variable $\phi(x;y;t)$ which assumes the value 0 if ϕ is constant inside a circle of radius ϕ centered in $(x;y)$, otherwise $\phi(x;y;t) = 1$ (i.e., $\phi(x;y;t) = 1$ only if the ϕ -ball centered in $(x;y)$ contains a portion of the front). The corresponding definition is

$$L(t) = \lim_{\phi \rightarrow 0} \frac{1}{\phi} \int_{-1}^1 dx \int_{-1}^1 dy \phi(x;y;t) \quad (5)$$

Then the average velocity and length are $v_f = \langle v(t) \rangle$ and $L_f = \langle L(t) \rangle$, where $\langle \cdot \rangle$ indicates a time average.

The geometrical optics limit can be formulated in terms of the evolution of a scalar field, $G(r;t)$, with the iso-scalar surface $G(r;t) = 0$ representing the front, i.e., where $G > 0$ there is inert material and where $G < 0$ only the fresh one is present. The evolution of G is ruled by the so-called G-equation [6,12,25-27]

$$\frac{\partial G}{\partial t} + u \cdot \nabla_x G = \sigma \nabla_x^2 G \quad (6)$$

The analytical treatment of this problem is not trivial at all, and also for relatively simple cases (e.g., shear flows) it is necessary to resort to numerical analysis.

Recently Majda and collaborators [15,26] pointed out that there are situations in which the G-equation fails in reproducing the front speed of the original reaction-advection-diffusion model. Indeed, in some systems the exact treatment of Eq. (1) in the limit $\epsilon \rightarrow 0$, $D_0 \rightarrow 0$ with $D = \epsilon \text{const}$ does not lead to the same results of the G-equation. However, for the application we are interested in the study of the G-equation is still physically relevant [15].

In this paper we consider the two-dimensional cellular flow, originally introduced in Ref. [28] to mimic roll patterns in Rayleigh-Bernard convection,

$$\begin{aligned} u_x(x;y;t) &= U \sin\left(\frac{2\pi}{L}x + B \sin(\omega t)\right) \cos\left(\frac{2\pi}{L}y\right) \\ u_y(x;y;t) &= U \cos\left(\frac{2\pi}{L}x + B \sin(\omega t)\right) \sin\left(\frac{2\pi}{L}y\right) \end{aligned} \quad (7)$$

where U is the flow intensity, L the roll size (in the following, for simplicity, $L = 2$) and the term $B \sin(\omega t)$ mimics the lateral oscillations of the roll pattern, which are produced by the oscillator instability [28]. We are interested both in the steady case, $B = 0$, and in the unsteady one, $B \neq 0$, where chaotic Lagrangian trajectories appear [17,28].

In the steady case, it is natural to expect that the front speed can be expressed according to the following relation [5,25]

$$v_f = v_0 \frac{U}{v_0} \quad (8)$$

Our aim will be to determine the shape of the function

Let us now briefly recall some known results on front propagation in cellular flows. To our knowledge the first study dates to the work of Ashurst and Sivashinsky [32] who showed that for high values of U the geometry of the front becomes rather complicated due to the formation of pockets of fresh material, i.e., islands of unburnt material generated behind the front. Aldredge [25] studied the dependence of v_f on U , finding, for large U , an almost linear dependence. Moreover, he compared the results with the relation [29]

$$v_f = v_0 = e^{d(U_{rms} = v_f)} \quad (9)$$

where $U_{rms} = U/\sqrt{2}$ is the root mean square velocity, and d and σ two parameters depending on the flow. The expression (9) has been originally proposed by Yakhot [30] and Sivashinsky [31] with $\sigma = 2$ and $d = 1$ for (multi-scale) turbulent flows. Such a formula has been frequently used in literature, also for non turbulent flows and various values of σ have been reported [5,25,29].

Concerning the results of Aldredge he found a fairly good agreement with the numerical estimations of v_f by employing expression (9) with $\sigma = 2$ and $d = 1/\sqrt{2}$.

Ashurst [16] proposed a different behavior for v_f , namely

$$v_f = \frac{(1 + U)}{(a + bU)} \quad (10)$$

where a, b are fitting parameters.

As far as the unsteady case is concerned, most of previous works have studied a particular time dependence, i.e., with $U = U \cos(\omega t)$ and $B = 0$ in (7). In this time dependent flow there is no Lagrangian chaos, and the overall effect (as recognized by most of authors [32,19]) is to suppress the front wrinkling and consequently causing a strong bending of the front speed with respect to the steady case. This phenomenon has been quantitatively understood for the case of time dependent shear flows (i.e., $u = (U \sin(\omega t) \sin(y); 0)$) by Majda and collaborators [20]. The physical reason for the damping has been understood in terms of the two time scales, t_o and t_w , respectively the period of oscillation and the "wrinkling" time, that is the time the front needs to reach the maximum speed stationary shape. If $t_o < t_w$ the front wrinkles, with the consequent speed enhancement. If $t_o > t_w$ the front has no time to experience the maximum enhancement and consequently the speed is damped with respect to the steady case. However, the time dependence considered in this paper (7) may, in principle, induce opposite effects. Indeed the possibility to transfer material from one cell to the adjacent may be enhanced with respect to the time independent case by varying ω (as found in particles transport [33,35]). Moreover, it is interesting to investigate the possible role of Lagrangian chaos on the front dynamics.

III. STATIONARY CELLULAR FLOW

Due to the spatial periodicity of the flow, after an initial transient, the front propagates quasi-steadily and periodically in time (with period T). In Fig. 1 a typical time series of the instantaneous velocity $v(t)$ is reported: peaks occur when the front length is maximal. The front speed, v_f , is obtained as an average over a period, $v_f = \langle v(t) \rangle_T$. Since the interface is sharp (being $(x;y)$ a two-valued function), we can easily track the farther edge of the interface between product and fresh material $(x_M(t); y_M(t))$. This is defined as the rightmost point (in the x -direction) for which $(x_M; y_M; t) = 1$. Thus we can also define a velocity

$$v_f = \lim_{t \rightarrow \infty} \frac{x_M(t)}{t} \quad (11)$$

which, since the front dynamics is periodic, is equivalent to the standard definition (see Fig. 1).

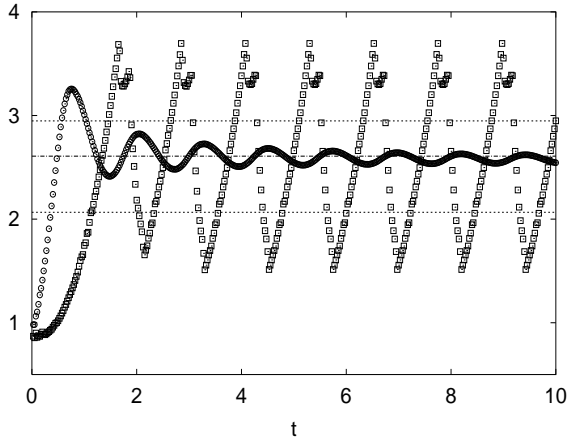


FIG. 1. Front speed, $v(t)$ as a function of time t measured in the standard way (4) (—), and as $x_M(t)=t$ (o). The three straight lines represent the average speed, the lower and upper bounds (see text). The system parameters are $U = 4$, $v_0 = 1$ and $L = 2$.

In Fig. 2 we show some snapshots of the front at various times. It is possible to see cusps and pockets (islands) of unburnt reactants left behind the front edge. At high field intensity a trail of pockets is formed.

Let us now try to understand the behavior of v_f as a function of U , providing an approximate expression for the adimensional function β . As far as we know, apart from very simple shear flows (for which $\beta(U) = U + 1$) [20], there are no methods to compute $\beta(U)$ from first principles. Mainly one has to resort to numerical simulations and phenomenological arguments. For the cellular flow under investigation, a simple argument can be provided to obtain an upper and a lower bound to v_f by mapping the front dynamics to a one-dimensional problem.

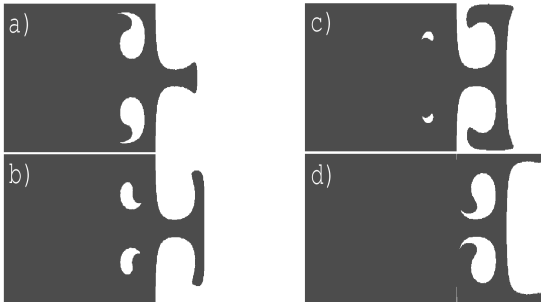


FIG. 2. Snapshot of the front shape with time step $T=8$, where T is the period of the front dynamics, for $v_0 = 0.5$, $U = 4$, $B = 0$ and as usual $L = 2$.

The strategy is to devise an equation for the edge point evolution (see Fig. 3). Asymptotically, in the cell $[0; 2] \times [0; 2]$ the point $(x_M(t); y_M(t))$ essentially moves in the right direction along the separatrices, so that $y_M(t)$ practically assumes values close to 0 or 2 . Moreover, it is clear from Eq. (11) that one needs just x_M in order to compute v_f , so one can reduce the edge dynamics to the

1d-problem

$$\frac{dx_M}{dt} = v_0 + U \langle j \sin(x_M(t)) \rangle \quad (12)$$

where the second term of the r.h.s. is the horizontal component of the velocity field and $\langle \cdot \rangle$ takes into account the average effect of the vertical component of the velocity field for the edge evolution. By solving (12) in the interval $x_M \in [0; 2]$ one obtains the time, T , needed for x_M to reach the end of the cell. Hence the front speed is given by $v_f = 2/T$

$$\beta(U) = \frac{2}{T} = \frac{2}{\int_0^2 \frac{1}{v_0 + U \langle j \sin(x_M(t)) \rangle} dx_M} \quad (13)$$

Note that (13) is valid only for $U \geq 1$, which is the regime we are interested in. We have taken $\beta = 1$ for the upper bound and $\beta = 1/2$ (which is the average of $\langle j \cos(y) \rangle$ in $[0; 2]$) for the lower bound. We have also numerically computed, for a particular set of parameters, the time average of $\langle j \cos(y_M(t)) \rangle$ along the path (see Fig. 3) obtaining 0.89 . With this value one has an impressive agreement with the measured v_f see Fig. 4. This is an indication that the average of $\langle j \cos(y_M(t)) \rangle$ depends on U and v_0 very weakly.

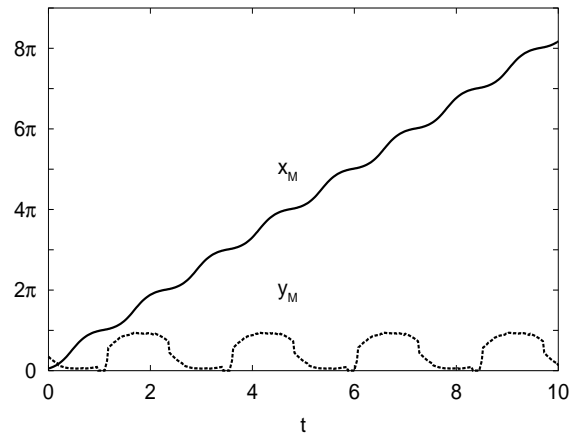


FIG. 3. Time evolution of the edge point: $x_M(t)$ and $y_M(t)$. The simulation parameters are the same of Fig. 1.

Previous studies [25] reported an essentially linear dependence of the front speed on the flow intensity, i.e., v_f / U for large U , which is not too far but definitely different from our result. A rigorous bound has been obtained in Ref. [36]:

$$v_f \geq U = \ln(1 + U/v_0) \quad (14)$$

As one can see from Fig. 4 the lower bound (14) seems to be closer to the numerical data than the one obtained with $\beta = 1/2$ in (13).

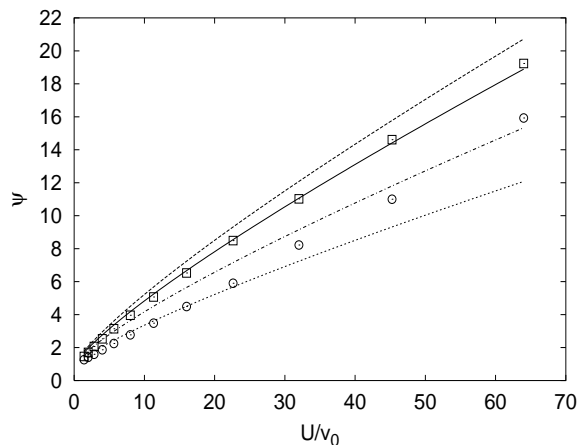


FIG. 4. The measured v_f ($U=v_0$) as a function of $U=v_0$ (2), the formula (9) with $\alpha=2$ and $d=1=2$ (o), the function for $\alpha=1; \beta=2$ (dashed and dotted lines) and for $\alpha=0.89$ (solid line). The dashed-dotted line is the bound (14).

From Eq. (13) or, equivalently from Eq. (14) for $U=v_0$ one has: $v_f = U \ln(U)$ which corresponds to (9) with $\alpha=1$. It is worth to stress that (9) has been proposed for flows with many scales, while in the system under investigation only one spatial scale is present. Therefore, in order to understand this point, we investigate now the possible role of small spatial scales.

A. Effect of small scales

We consider the following generalization of the velocity field (7):

$$\begin{aligned}
 u_x(x;y;t) &= U \sin\left(\frac{2}{L}x\right) \cos\left(\frac{2}{L}y\right) \\
 &+ Q \sin\left(\frac{2}{L}kx + \phi_1\right) \cos\left(\frac{2}{L}ky + \phi_2\right) \\
 u_y(x;y;t) &= U \cos\left(\frac{2}{L}x\right) \sin\left(\frac{2}{L}y\right) \\
 &- Q \cos\left(\frac{2}{L}kx + \phi_1\right) \sin\left(\frac{2}{L}ky + \phi_2\right)
 \end{aligned} \quad (15)$$

where $U=Q=1$, ϕ_1, ϕ_2 indicate the (time-independent) phase differences between the two contributions to the velocity field, and k is an integer giving the ratio between the two spatial scales. In Fig. 5 we present a snapshot of the front for two different values of the parameters. By comparing with Fig. 2 is evident the presence of small structures in the front due to smaller scales in u . We computed v_f for different k taking $U=Q$ constant, and compared with the one scale flow ($Q=0$). The results are summarized in Fig. 6, where v_f is rescaled with v_0 and reported as a function of $U_{rms}=v_0$ ($U_{rms} = U \sqrt{1+Q^2}=U^2=2$). As one can see, they almost collapse onto a single curve together with the one scale results (see Fig. 6).

The physical information one can extract from the above result is that the front speed is essentially determined by the large scale behavior of the velocity field, e.g. the absence of open channels can be more important than the detailed multi-scale properties of the flow [16].

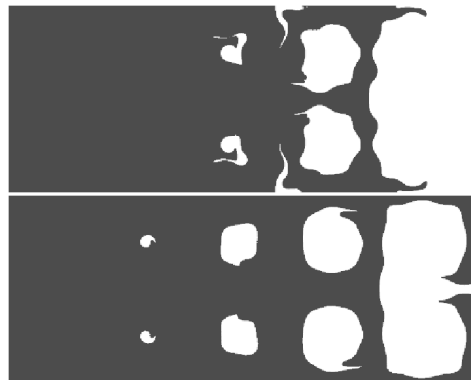


FIG. 5. Images of the burnt area (black) for $U=6, Q=3$ (above) and $U=10, Q=2$ (below) with $k=5$, where $v_0=0.5$. The different scales are clearly visible.

It is worth to conclude this section with some general remarks. For the one scale flow in the steady case, we found that $v_f = U \ln(U)$ as the flow intensity U (or U_{rms} equivalently) is very large. Such a kind of behavior corresponds to the large U limit of the Yakhot like formula (9) with $\alpha=1$. Our results show that the main effect of the small scales is to renormalize the stirring intensity. Indeed from Fig. 6 one can see that once taken into account U_{rms} all the curves roughly collapse.

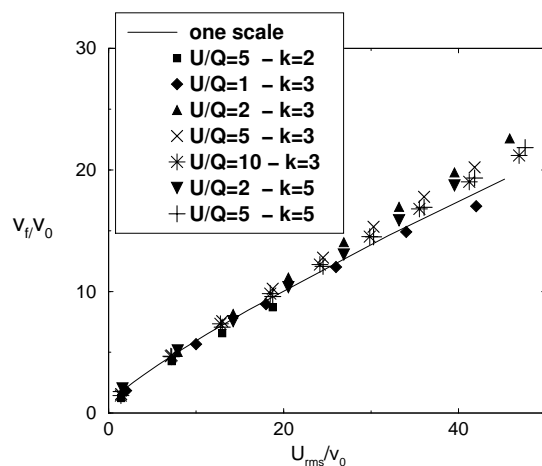


FIG. 6. Front velocities $v_f=v_0$ as a function of $U_{rms}=v_0$ for the flow (15) for various k -values and $U=Q$ ratios. The data refers to $v_0=0.5$.

From Figs 5 and 6 one can see that the introduction of small scales on u causes a roughening of the front shape only at the same scales of the velocity fields, and has

just a minor effect on the front speed. The problem of the effect of small scales on u on the front wrinkling had been studied also by Denet [34] in the context of the flame propagation equation (FPE) (which is similar to the Kardar-Parisi-Zhang equation). In this case the small scales influence on the large scale motion seems to be important. However, the relation between Eq.(1) and the FPE is not straightforward and the experimental results are not very clear so the general problem is still open.

Coming back to Fig. 6, it seems that, for the functional dependence of v_f on U_{rms} , a major role is played by the large scale structures of the flow. The fair agreement of data with formulas like (9) can be interpreted as follows. At large stirring intensities, i.e., large U_{rms} , one must have roughly a linear behavior, $v_f \propto U_{rms}$, apart from small corrections which carries the flow details. Consider two limiting behaviors: (steady) shear flows, which is the most favorable situation for the front speed enhancement, one exactly has $v_f / U_{rms} = 20$; for (steady) cellular flow, which is the worst situation, we obtained $v_f / U_{rms} = \ln(U_{rms})$. In a generic flow it is reasonable to expect a behavior in between, which can be fitted by (9) with the appropriate λ and d .

IV. NON-STATIONARY CELLULAR FLOW

Let us now consider the problem of front propagation in the time dependent cellular flow (7) (i.e., $B; \lambda \neq 0$). We are mainly interested in addressing the two following issues. First, since trajectories starting near the roll separatrices typically have a positive Lyapunov exponent, it is natural to ask about the role of Lagrangian chaos on front propagation (see IV A). Second, from previous works [33,35] we know that for the time dependent flow (7) transport is strongly enhanced, therefore it is interesting to see if the same happens for the front speed. As we will see in subsection IV B, the situation is much more subtle.

A. Transient dynamics of front propagation

It is well known that passive particles, $r(t)$ advected by the flow (7) with $B; \lambda \neq 0$ (i.e., $\underline{r} = u(r(t); t)$) display Lagrangian chaos, i.e., they have a positive Lyapunov exponent [17,28]. A direct consequence of having chaotic Lagrangian trajectories is the exponential growth of material lines and of passive scalar gradients [17]. In other words, the long time evolution of a (passive) material line of initial length l_0 increases exponentially in time as

$$l(t) \approx l_0 e^{\lambda t} \quad (16)$$

Where λ is the first generalized Lyapunov exponent, i.e.,

$$\lambda = \lim_{t \rightarrow \infty} \frac{1}{t} \ln \frac{|j r(t) j|}{|j r(0) j|} ;$$

which is in general larger than the maximum Lyapunov exponent. The average in the previous equation is taken along the Lagrangian trajectories.

In the presence of molecular diffusivity, the exponential growth of $l(t)$ arrests due to diffusion [17] and, as a consequence, chaos is just a transient [37]. As we will see for the reacting scalar something very similar happens.

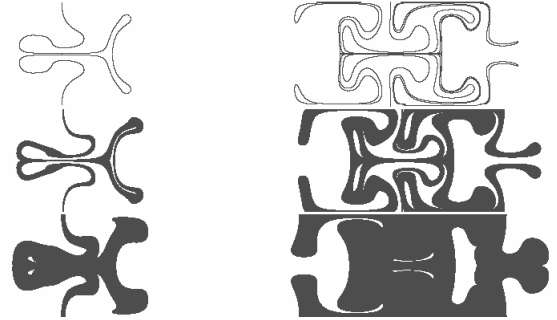


FIG. 7. Snapshot at two successive times, $t = 3.6$ and 7.5 , of the evolution of passive (top) and reactive line of material for two values of v_0 (middle $v_0 = 0.7$ and bottom $v_0 = 2.1$) for $U = 1.9$, $B = 1.1$ and $\lambda = 1.1U$. The initial condition is a straight vertical line in $x = 0$.

Let us compare the evolution of material lines in the passive and reactive case (see Fig. 7). Looking at the pictures one can see that while in the passive case structures on smaller and smaller scales develop (due to stretching and folding), in the reactive one after a number of folding events the formation of structures on smaller scales is stopped as a consequence of reaction (Huygens dynamics). Indeed due to reaction one has the "merging" of the interfaces between the two phases. This phenomenon is responsible for the formation of pockets [32,25]. Of course, the "merging" is more and more efficient as v_0 increases (compare the middle and lower pictures of Fig. 7).

In Fig. 8 we show the time evolution of the line length, $L(t)$, as a function of t for the passive and reactive material at different values of v_0 . It is easy to see that while at small times either passive and reactive scalar lines grow exponentially with a rate close to λ , at large time, due to the merging mechanism, the reacting ones stop after a transient time, t^* , which depends on v_0 . In the stationary situation the front length varies periodically with an average value which depends on v_0 . A very rough argument to estimate the duration of the transient time, t^* , is the following. Due to Lagrangian chaos one has stretching and folding so that two initially separated part of the line (e.g. originally of distance l_0) start to become closer and closer, roughly as $l_0 \exp(-\lambda t)$. When such a distance becomes of the order of $v_0 t$ the merging takes place. So that to leading order one can estimate

$$t^* \approx \frac{1}{\lambda} \ln \frac{l_0}{v_0} \quad (17)$$

When the system reaches its asymptotic state ($t > t_c$) both the spatial and temporal structures of the flow become periodic. Now we will analyze the influence of the flow time dependence on the asymptotic average front speed in order to understand whether it is enhanced or depleted with respect to the steady case. Moreover, we will discuss the possible (residual) effects of Lagrangian chaos in the asymptotic regime.

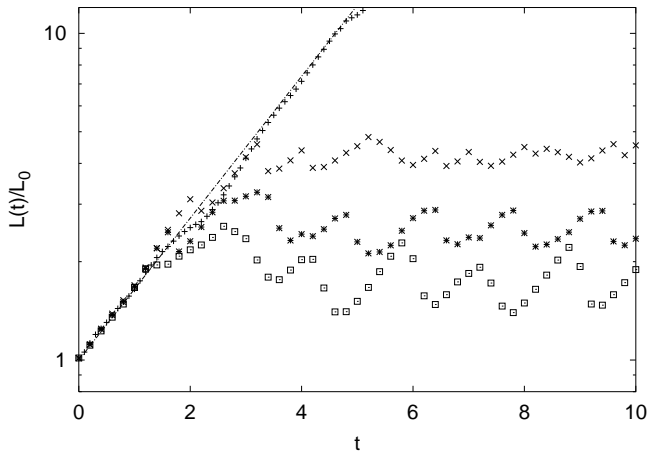


FIG. 8. $L(t)/L_0$ as a function of time for $U = 1.9$, $B = 1.1$ and $\omega = 1.1U$ for the passive (+) and reactive case at different values of v_0 , from top $v_0 = 0.3$ (*); 0.5 (x); 0.7 (2). The straight line indicates the curve $\exp(t)$ with slope 0.5 , which has been directly measured by means of Lagrangian dynamics of (7).

B. Front speed dependence on the frequency

In the context of passive particles transport, the time dependence in the flow (7) has dramatic effects on the effective diffusion constant, D_e [33,35]. It has been found that the eddy diffusivity constant $D_e(\omega)$ displays a complex behavior with resonant-like patterns in which the values of $D_e(\omega)$ are orders of magnitude larger than the stationary-flow value, $D_e(0)$ [38]. The physical mechanism responsible for the resonances is related to the interplay between the oscillation period of the separatrices and the circulation time inside the cell. It happens that circulation and oscillation "synchronize" producing a very efficient and coherent way of transferring passive particles from one cell to the other leading to the "resonances", i.e., the extremely high values of $D_e(\omega)$, which in the limit $D_0 \rightarrow 0$ give rise to anomalous diffusion [33]. Therefore, it is interesting to wonder whether the time dependence of the flow induces a more efficient transport of burnt material and, as a consequence, an enhancement of the front speed with respect to the steady case.

In Fig. 9 we report $v_f(\omega)$ as a function of $\omega = \omega/U$ (due to the choice $L = 2$, U naturally defines an intrinsic frequency for the cellular flow). As one can see, $v_f(\omega)$

varies both above and below the time independent value, $v_f(0)$. However, the range of variability of the front speed is very small compared to what happens to the diffusion constant, varying about 30% above or below the time independent value $v_f(0)$. If one changes the value of v_0 then the curve display a small shift up (increasing v_0) or down (decreasing v_0) with some slight variation of the values of the peaks. This behavior is very robust with respect to changes of the flow parameters (U and B).

A direct inspection of the figures shows that $v_f(\omega)$ is very close to be a piece-wise linear function of ω . In particular, we found that the slope is given by U multiplied by a rational number. Such a kind of behavior closely resemble the frequency locking phenomenon [21,22]. Frequency locking naturally arises in some non linear oscillators which are periodically forced, when the oscillator synchronizes its frequency to the one of the periodic force.

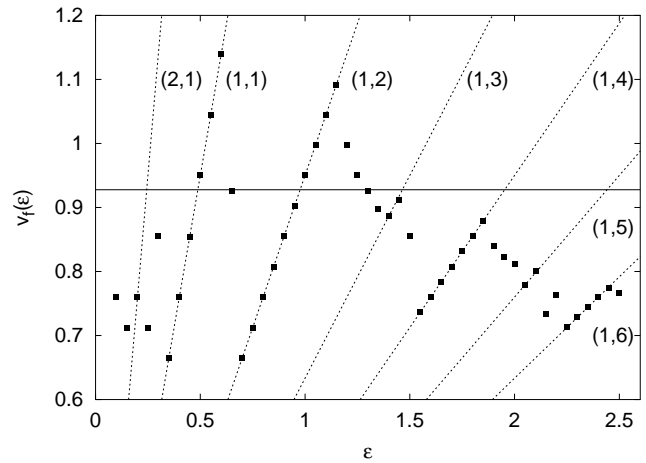


FIG. 9. $v_f(\omega)$ as a function of $\omega = \omega/U$, for the flow (7) with $U = 1.9$, $v_0 = 0.2$ and $B = 1.1$. The straight horizontal line indicates the front speed for the steady case $B = 0$. The dashed lines indicate the curve $N = M U$ for different $(N; M)$ integers.

On the basis of the frequency locking phenomenology, the front speed dependence on the frequency of oscillation of the separatrices can be explained by a very simple argument. At large times, $t > t_c$, the front is time and space periodic. This means that if the equation $F(x; y) = 0$ describes the front shape at time t , then at time $t + T$ it has the same shape but shifted in the x -direction, i.e. $F(x + S; y) = 0$, being S and T the spatial and temporal periods respectively. Due to the spatial periodicity of the flow $S = 2N$ (where N integer). Now one expects T to be a multiple of the oscillation period $T_0 = 2/\omega$ so that: $T = M T_0$ (with M integer). This is confirmed by the simulations. On the other hand, the front speed is nothing but S/T so that

$$v_f = \frac{S}{T} = \frac{2N}{M T_0} = \frac{N}{M} \omega = \frac{N}{M} U ; \quad (18)$$

which is indeed the behavior we observed in Fig. 9. Varying ν the periods $S = 2M$ and $T = NT_0$ with a given M and N can lose their stability so that a new couple of $N;M$ values is selected. This explains the presence of different linear behaviors.

Of course such kind of frequency dependence is mainly due to the spatial and temporal periodicity of the flow. From the point of view of front propagation, even if the dependence of the front speed as a function of the frequency is much more complex than that for shear flows [20], the inequality $v_f \geq U + v_0$ makes the relative variations of the front speed to be less dramatic than the ones of the diffusion constant.

Let us remark that by generalizing the one dimensional model (12) to the time dependent case we have been able to qualitatively reproduce the behavior of the front speed dependence on the frequency. In appendix B we report some more details on the frequency locking phenomenon and on the one-dimensional model.

C. Velocity and length dependence on v_0

In Section IV A we studied the effects of Lagrangian chaos on the transient dynamics of front propagation. Here we want to understand if also in the asymptotic regime, in which chaos is suppressed by the merging mechanism, remains some effects due to the chaotic nature of the transport dynamics.

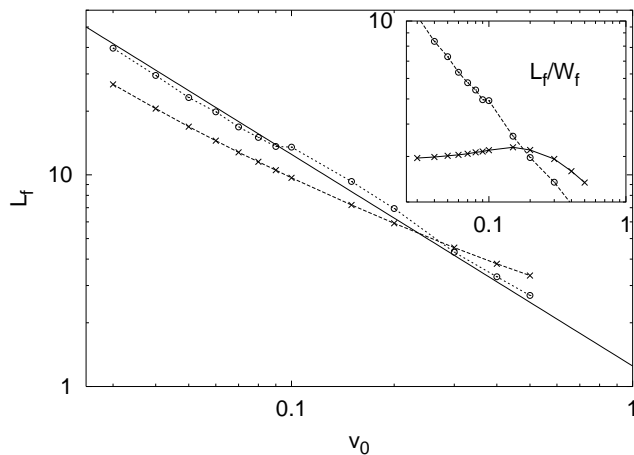


FIG. 10. The average front length $L_f=L$ as a function of v_0 for the time dependent flow (○), with $U = 1.9$, $B = 1.1$, $\nu = 2.09$ and the time independent case (×) with $U = 1.9$. The straight line indicates the $1=v_0$ behavior. In the inset it is displayed the ratio $L_f=W_f$ as a function of v_0 for the time dependent (○) and independent (×) cases.

An immediate consequence of Eq. (17) is that the asymptotic front length (5) behaves as $L_f \propto v_0^{-1}$. Indeed,

$$L_f \propto L e^{-t} \frac{L^2}{v_0}; \quad (19)$$

which is in fairly good agreement with the simulations (see Fig. 10). In this respect it is interesting to note that in the steady case a different scaling can be seen. Of course, (19) is expected to hold only for small values of v_0 . However, this kind of scaling is also present in a simple non chaotic shear flow. Indeed, for the shear flow ($u_x = U \sin(y)$; $u_y = 0$) one has $v_f = U + v_0$ and at the same time, from Eq. (3), $v_f = L_f v_0$ so that $L_f = 1+v_0/U$ for $U=v_0$. Therefore, the scaling $L_f \propto v_0^{-1}$ is not peculiar of flows with chaotic transport. However, in presence of Lagrangian chaos the scaling $L_f \propto v_0^{-1}$ holds.

Another quantity linked to the structure of front is the width of the front, W_f , i.e., the extension of the region in which burnt and unburnt material coexist. Such an observable can be defined as follows [23]. First we define a measure $\chi(x)$

$$\chi(x) = \frac{\int_{-\infty}^{\infty} \tilde{\chi}(x) dx}{\int_{-\infty}^{\infty} \tilde{\chi}(x) dx}; \quad (20)$$

where $\tilde{\chi}(x) = \frac{1}{L} \int_0^L \chi(x;y) dy$. Then we considered as a measure of the width the standard deviation obtained with such a measure, i.e.,

$$W_f = \frac{\int_{-\infty}^{\infty} \chi^2(x) dx}{\left(\int_{-\infty}^{\infty} \chi(x) dx \right)^2} \quad (21)$$

For a simple shear flow W_f and L_f display the same kind of dependence on v_0 (actually they are proportional). In a generic chaotic flows one can expect that the Lagrangian transport induces an increasing of the front length, but has minor influence in determining its width, or eventually it can decrease it because of the enhanced (chaotic) mixing. This is indeed what one observes in the inset of Fig. 10, where we show the ratio $L_f=W_f$ both for the stationary (non-chaotic) and the time-dependent (chaotic) flow. For the latter case this ratio diverges for very small v_0 values as a signature of chaos. From a physical point of view the ratio $L_f=W_f$ is an indicator of the "spatial complexity" of the front. Indeed it indicates the degree of wrinkling of the front with respect to the size of the region in which the front is present. The presence of chaos manifests in a divergence of $L_f=W_f$ for small v_0 values. In some sense we can say that the temporal "complexity" of Lagrangian trajectories converts in the spatial "complexity" of the front.

We conclude this section by comparing the front speed in the time-dependent and time-independent flow as a function of v_0 . As one can see from Fig. 11 one realizes that for very small v_0 the time dependent flow leads to an increase of the velocity due to the more efficient way to transfer material from one cell to the other. At large values of v_0 the time-independent flow has a larger front speed than the time-dependent one.

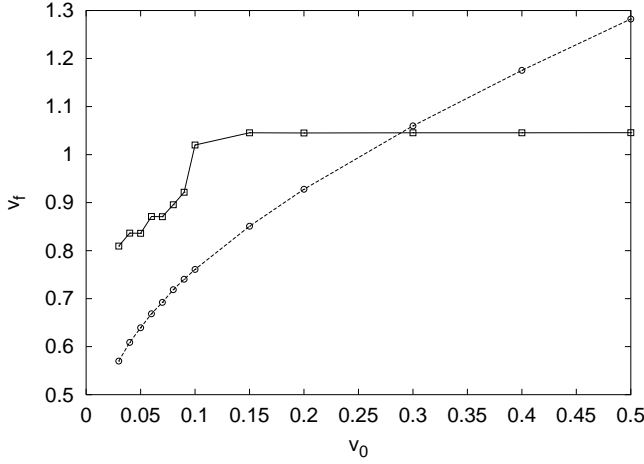


FIG. 11. v_f versus v_0 for the time dependent case with $U = 1.9$, $B = 1.1$, $\lambda = 1.1U$ (2) and for the time independent case with $U = 1.9$ and $B = 0$ (1).

This is another consequence of the mode-locking of the dynamics, which maintains constant the value of v_f .

V. FINAL REMARKS

In this paper we studied the thin front propagation in steady and unsteady cellular flows. In particular, we investigated the speed and the spatial structure of the front (mainly the front length L_f and width W_f) as a function of the system parameters.

Concerning the front speed, we proposed a simple model (without adjustable parameters) able to reproduce most of the results, and capable, in the steady case, to give also a quantitative description of the system. The front speed is essentially determined by the large scales behavior of the velocity field. Indeed by adding small scales contributes to the main flow, v_f does not drastically change. In fact, in the steady case, asymptotically the front speed as a function of the stirring intensity U (or U_{rms} equivalently) behaves like $U = \ln(U)$, which corresponds to the large U limit of the Yakhot like formula (9) with $\beta = 1$. The fair agreement of data with such a class of functions can be due to the fact that at large stirring intensities one must have roughly a linear behavior $v_f \sim U_{rms}$ apart from small corrections which carries the flow details. For general time dependent flows it could be present decorrelation effects leading to a depletion of the front speed, but we expect that the qualitative behavior should remain similar to the steady case.

As far as the time dependent cellular flow here considered is concerned, it is important to remark that the effect of chaos on the front propagation is limited to a transient, in which the front behavior is close to the passive scalar case. Asymptotically, the reacting term induces a drastic regularization on the front evolution, suppressing the effects of small scales and Lagrangian

chaos. Indeed after the transient the front propagates periodically and, as a consequence of the particular time dependence here considered, displays a frequency locking phenomenon. The only asymptotic effect of Lagrangian chaos is in the structure of the front which is more and more wrinkled as v_0 approaches to zero. On the contrary in the case of steady velocity fields (regular Lagrangian motion) the degree of irregularity does not change with v_0 . As an indicator of the spatial "complexity" of the front we used the ratio between the front length and the width, L_f/W_f which is large (diverging as $v_0 \rightarrow 0$) for the unsteady case and is roughly constant for the steady one.

ACKNOWLEDGMENTS

We gratefully thank A. Magoli and A. Celani for discussions and correspondences. This work has been partially supported by the INFN Parallel Computing Initiative and MURST (Compendio Fisica Statistica e Teoria della Materia Condensata). M.C., D.V. and A.V. acknowledge support from the INFN Center for Statistical Mechanics and Complexity (SMC).

APPENDIX A: NUMERICAL ALGORITHM

In numerical approaches one is forced to discretize both space and time. We introduce a lattice of mesh size Δx and Δy (for the sake of simplicity we assume $\Delta x = \Delta y$) so that the scalar field is defined on the points $\mathbf{x}_{n,m} = (n\Delta x; m\Delta y)$: $\phi_{n,m}(t) = \phi(n\Delta x; m\Delta y; t)$. The time discretization implies a discretization of the dynamics. Looking at the G-equation (6) one immediately recognize two different terms: the advection term $\mathbf{u} \cdot \nabla \phi$ and the "geometrical" term $v_0 \nabla^2 \phi$. The first is the responsible for the transport properties of the flow, while the second accounts for the optical behaviour of the front (that locally propagates in a direction perpendicular to the front, and with a bare velocity v_0). Once has been discretized, the Lagrangian evolution is given by a conservative map (in 2d the map is symplectic due to the incompressibility of the flow)

$$\mathbf{x}(t + \Delta t) = \mathbf{F}^{\Delta t}(\mathbf{x}(t)); \quad (A1)$$

where the map $\mathbf{F}^{\Delta t}$ is the Lagrangian propagator. Therefore, given the field at time t one can compute the field at time $t + \Delta t$ using a two steps algorithm:

- 1) using the Lagrangian propagator, $\mathbf{F}^{\Delta t}(\mathbf{x})$, one evolves each point of the interface between burnt and unburnt region;
- 2) at each point of the evolved interface one constructs a circle of radius $v_0 \Delta t$, obtaining the new frontier as the envelope of the circles.

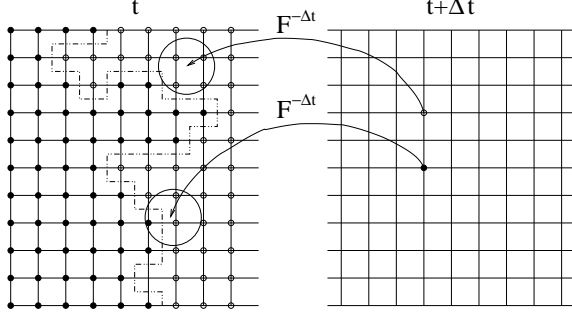


FIG. 12. Pictorial scheme of the numerical algorithm for the geometrical optics limit.

To implement numerically such an algorithm one can proceed as follows: starting on a grid point, $x_{n,m}$, of the scalar field at time $t + \Delta t$ one applies the backward evolution arriving at the point $y = F^{-\Delta t} x_{n,m}$ at time t . Around this point we construct the circle of radius $v_0 \Delta t$. If in this circle there is at least one burnt point of the scalar field at time t , we set $x(x_{n,m}; t + \Delta t) = 1$ otherwise $x(x_{n,m}; t + \Delta t) = 0$.

It is worth to note that one has to care about the radius of circle $v_0 \Delta t$ that has to be much larger than the grid-size Δx .

Typical values used in our simulation are $\Delta t = 0.02$, $\Delta x = 2048$. The Lagrangian propagator $F^{-\Delta t}(x)$ had been computed with a 4-th order Runge-Kutta algorithm.

APPENDIX B: FRONT SPEED LOCKING

Frequency Locking arises in many physical systems ranging from Josephson-junction arrays to chemical reactions and non linear oscillators [21]{23}. The basic mechanism is a resonance effect between two oscillators or when an oscillator is coupled with an external periodic forcing. In the last case the system synchronizes with the external forcing making its internal frequency commensurable with the external one. Almost all the systems displaying frequency locking can be mapped (by means of appropriate transformation) to a sort of damped forced non linear oscillators [21], a typical and very well studied example is:

$$\frac{d^2}{dt^2} + \frac{d}{dt} + \sin(\phi) = \epsilon + \cos(\Omega t) \quad (B1)$$

The solution $\phi(t)$ is periodic and the frequency, i.e., the average angular velocity, turns out to be:

$$\lim_{t \rightarrow \infty} \frac{d\phi}{dt} = \frac{M}{N} \quad (B2)$$

with $M; N$ integers. Moreover, if (B2) is realized for a certain set of the parameters there always exist an entire

interval around their values where (B2) holds with the same values of M and N . This kind of behavior persists also when $\epsilon = 0$ and for other kind of non linear terms (i.e. the third term of the l.h.s.). An exhaustive description of such a phenomenon can be found in Refs. [22].

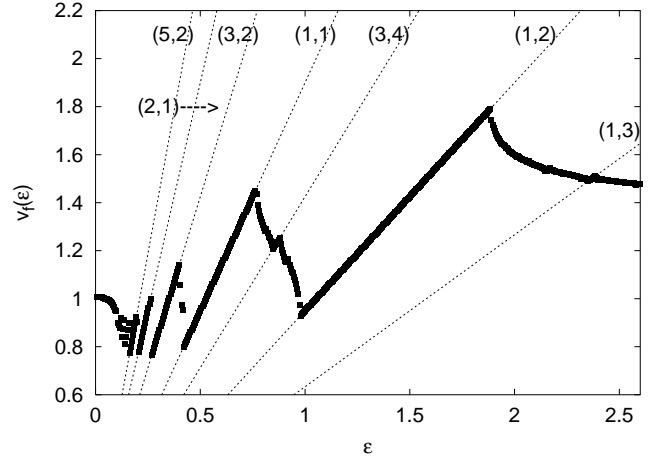


FIG. 13. $v_M(\epsilon)$ as a function of $\epsilon = U$, for the model (B3) with $U = 1.9$, $v_0 = 0.2$ and $B = 1.1$. The dashed lines indicate the curve $N = M U$ for different $N; M$ integers.

Coming back to our system, it is very hard to derive an effective equation such as (B1). In order to understand the arising of locking in the front speed, we consider the generalization of the 1d-model (12) to the time dependent case:

$$\frac{dx_M(t)}{dt} = v_0 + U \text{jsin}(x_M + B \sin(\Omega t)) \quad (B3)$$

Note that in principle one should also take into account the dynamics of y_M , but for the sake of simplicity we present just the y -independent version of the model. We will see that this model is able to reproduce behaviors qualitatively similar to the ones observed in the simulations and it can be reduced to an equation similar to (B1).

By directly integrating (B3) one obtains the same qualitative results for the front speed, this is well evident by comparing Fig. (13), where we show $v_M(\Omega) = \lim_{t \rightarrow \infty} \frac{1}{t} x_M(t) = \Omega$ versus Ω , with Fig. 9. By a simple change of variables $z(t) = x_M(t) + B \sin(\Omega t)$ Eq. (B3) can be reduced to

$$\frac{dz(t)}{dt} = v_0 + U \text{jsin}(z) + B \Omega \cos(\Omega t) \quad (B4)$$

which is similar to (B1), and for which frequency locking has been studied in details. In this direction it is interesting to quote a recent work [39] which has studied the problem of locking in a model very similar to (B4) with the addition of noise. They found that the locking phenomenon is rather robust under the effect of noise and,

Moreover, it gives rise to resonances in the diffusion coefficient. All these results are qualitatively very similar to the behavior of the system here studied.

-
- [1] E. R. Abraham, "The generation of plankton patchiness by turbulent stirring", *Nature* 391, 577 (1998); E. R. Abraham, C. S. Law, P. W. Boyd, P. W. S. J. Laverender, M. T. Maldonado and A. R. Bowie, "Importance of stirring in the development of an iron-fertilized phytoplankton bloom", *Nature* 407, 727 (2000).
- [2] J. Ross, S. C. M. Muller, and C. Vidal, "Chemical waves", *Science* 240, 460 (1988); I. R. Epstein, "The consequences of imperfect mixing in auto-catalytic chemical and biological systems", *Nature* 374, 231 (1995).
- [3] F. A. Williams, *Combustion Theory* (Benjamin Cummings, Menlo Park 1985).
- [4] S. Maham and J. Xin, "Global solutions to a reactive Boussinesq system with front data on an infinite domain", *Comm. Math. Phys.* 199, 287 (1998).
- [5] P. D. Ronney, "Some open issues in premixed turbulent combustion", in *Modeling in Combustion Science*, pp. 3-22, Eds. J. Buckmaster and T. Takeno (Springer-Verlag Lecture Notes in Physics, 1994).
- [6] N. Peters, *Turbulent combustion* (Cambridge University Press, 2000).
- [7] J. Xin, "Front Propagation in Heterogeneous Media", *SIAM Review* 42, 161 (2000).
- [8] A. J. Majda, and P. R. Kramer, "Simplified models for turbulent diffusion: Theory, numerical modelling and physical phenomena", *Phys. Rep.* 314, 237 (1999).
- [9] A. N. Kolmogorov, I. G. Petrovskii, and N. S. Piskunov, "Study of the diffusion equation with growth of the quantity of matter and its application to a biology problem", *Moscow Univ. Bull. Math.* 1, 1 (1937); R. A. Fischer, "The Wave of Advance of Advantageous Genes", *Ann. Eugenics* 7, 355 (1937).
- [10] A. C. Marti, F. Sagues and J. M. Sancho, "Front dynamics in turbulent media", *Phys. Fluids* 9, 3851 (1997).
- [11] M. Abel, A. Celani, D. Vergni and A. Vulpiani, "Front propagation in laminar flows", *Phys. Rev. E* 64, 046307 (2001).
- [12] A. R. Kerstein, W. T. Ashurst, F. A. Williams, "Field equation for interface propagation in an unsteady homogeneous flow field", *Phys. Rev. A* 37, 2728 (1988).
- [13] P. Constantin, A. Kiselev, A. Obembe and L. Ryzhik, "Bulk Burning Rate in Passive - Reactive Diffusion", *Arch. Rational Mechanics* 154, 53 (2000).
- [14] B. Audoly, H. Beresnytski and Y. Pomau, "Reaction diffusion en écoulement stationnaire rapide", *C. R. Acad. Sci.* 328, Serie II b, 255 (2000).
- [15] A. Bourloux and A. J. Majda, "An elementary model for the validation of flame approximations in non-premixed turbulent combustion" *Comb. Th. and Model.* 4, 189 (2000).
- [16] W. T. Ashurst, "Flame propagation through swirling eddies, a recursive pattern", *Comb. Sci. Tech.* 92, 87 (1993).
- [17] J. M. Ottino, *The kinematics of mixing: stretching, chaos and transport* (Cambridge University Press, 1989); A. Crisanti, M. Falconi, G. Paladin and A. Vulpiani, "Lagrangian Chaos: Transport, Mixing and Diffusion in Fluids", *La Rivista del Nuovo Cimento* 14, 1 (1991).
- [18] W. T. Ashurst, "Low-frequency effect upon Huygens front propagation", *Comb. Th. Model.* 4, 99 (2000).
- [19] B. Denet, "Possible role of temporal correlations in the bending of turbulent flame velocity", *Comb. Th. Model.* 3, 585 (1999).
- [20] B. Khouider, A. Bourloux and A. J. Majda, "Parameterizing the burning speed enhancement by small-scale periodic flows: I. Unsteady shears, flame residence time and bending", *Comb. Th. Model.* 5, 295 (2001).
- [21] M. H. Jensen, P. Bak and T. Bohr, "Complete devil's staircase, fractal dimension, and universality of mode-locking structure in the circle map", *Phys. Rev. Lett.* 50, 1637 (1983); "Transition to chaos by interaction and overlap of resonances, I: Circle maps", *Phys. Rev. A* 30, 1960 (1984).
- [22] A. Pikovsky, M. Rosenblum, and J. Kurths, *Synchronization: A Universal Concept in Nonlinear Sciences*, (Cambridge University Press, 2001).
- [23] R. Carretero-Gonzalez, D. K. Arrowsmith and F. Vivaldi, "Mode-locking in coupled map lattices" *Physica D* 103, 381 (1997).
- [24] D. Benedetto, E. Caglioti and R. L. Libero, "Non-trapping sets and Huygens principle" *Rairo-Math. Model. Num.* 33, 517 (1999).
- [25] R. C. Aldredge, "The Scalar-Field Front Propagation Equation and its Applications", in *Modeling in Combustion Science*, pp. 23-35, Eds., J. Buckmaster and T. Takeno (Springer-Verlag Lecture Notes in Physics, 1994); "Premixed Flame Propagation in a High-Intensity, Large-Scale Vortical Flow", *Comb. and Flame* 106, 29 (1996).
- [26] P. F. Embid, A. J. Majda and P. E. Souganidis, "Comparison of turbulent flame speeds from complete averaging and the G-equation", *Phys. Fluids* 7 (8), 2052 (1995).
- [27] R. M. McLaughlin and J. Zhu, "The effect of finite front thickness on the enhanced speed of propagation", *Comb. Sci. Tech.* 129, 89 (1997).
- [28] T. H. Solomon and J. P. Gollub, "Chaotic particle transport in time-dependent Rayleigh-Benard convection", *Phys. Rev. A* 38, 6280 (1988); "Passive transport in steady Rayleigh-Benard convection", *Phys. Fluids* 31, 1372 (1988).
- [29] A. R. Kerstein and W. T. Ashurst, "Propagating rate of growing interfaces in stirred fluids", *Phys. Rev. Lett.* 68, 934 (1992).
- [30] V. Yakhot, "Propagation velocity of premixed turbulent flame", *Comb. Sci. Tech.* 60, 191 (1988). M. Chertkov, V. Yakhot, "Propagation of a Huygens front through turbulent medium", *Phys. Rev. Lett.* 80, 2837 (1998).
- [31] G. I. Shivshinsky, "Cascade-renormalization theory of turbulent flame speed", *Comb. Sci. and Tech.* 62, 77 (1988).
- [32] W. T. Ashurst and G. I. Shivshinsky, "On flame propagation through periodic flow fields", *Comb. Sci. Tech.*

- 80, 159 (1991).
- [33] P. Castiglione, A. Mazzino, P. Muratore-Ginanneschi, A. Vulpiani, "On strong anomalous diffusion", *Physica D*, 134, 75 (1999). P. Castiglione, A. Crisanti, A. Mazzino, M. Vergassola, A. Vulpiani, "Resonant enhanced diffusion in time-dependent flow" *J. Phys A* 31, 7197 (1998).
- [34] B. Denechère, "Are small scales of turbulence able to wrinkle a premixed flame at large scale?", *Comb. Theory and Modelling* 2, 167 (1998).
- [35] T. Solomon, A. Lee, M. Fogelson, "Resonant lights and transient super-diffusion in a time-periodic, two-dimensional flow", *Physica D* 157 40 (2001).
- [36] A. Oberman, PhD Thesis Univ. of Chicago 2001.
- [37] A. K. Pattanayak "Characterizing the metastable balance between chaos and diffusion", *Physica D*, 148, 1 (2001); M. Giona, S. Cerbelli and A. A. drover "Geometry of Reaction Interfaces in Chaotic Flows", *Phys. Rev. Lett.* 88, 024501 (2002).
- [38] Y. Pomeau, "Dispersion dans un écoulement en présence de zones de recirculation", *C. R. Acad. Sci.* 301, 1323 (1985).
- [39] D. Reguera, P. Reimann, P. Hanggi and J.M. Rubi, "Interplay of frequency-synchronization with noise: current resonances, giant diffusion and diffusion-crests", *Europhys. Lett.* in press; arXiv:cond-mat/0112320